COPY

(2)

AD-A221 985

NTATION PAGE

Form Approved
OMB No. 0704-0188

1. AGENCY USE ONLY (Leave blank)	2. REPORT DATE	3. REPORT TYPE AND DATES COVERED
	90-05-09	Final 15Jan87 To 14Jan90

4. TITLE AND SUBTITLE
Physics and Techniques for the Investigation of the Properties of Ultra Small Systems

5. FUNDING NUMBERS
AFOSR-87-0148

6. AUTHOR(S)
J.M. Parpia & R.C. Richardson

AFOSR-TR- 90 0641

7. PERFORMING ORGANIZATION NAME(S) AND ADDRESS(ES)
Cornell University
Department of Physics, Clark Hall
Ithaca, NY 14853

8. PERFORMING ORGANIZATION REPORT NUMBER

9. SPONSORING / MONITORING AGENCY NAME(S) AND ADDRESS(ES)
AFOSR
Bldg #410
Bolling AFB
Washington, D.C. 20332-6448

10. SPONSORING / MONITORING AGENCY REPORT NUMBER
2306/C1

DTIC
ELECTE
MAY 29 1990
S D
D

11. SUPPLEMENTARY NOTES

12a. DISTRIBUTION / AVAILABILITY STATEMENT
Approved for public release
Distribution unlimited
NE

12b. DISTRIBUTION CODE

13. ABSTRACT *(Maximum 200 words)*

This program is directed toward the study of transport and non-equilibrium thermal effects in diverse miniaturized systems at low temperatures. The research ~~uses capabilities developed at Cornell to~~ fabricate, and probe, the behavior of materials without affecting their internal structure. The techniques extend our ability to characterize materials as well as to understand the effects of technology used in patterning and fabricating small devices. The techniques developed in this research should prove to be useful for the non-destructive evaluation of the properties of materials as well as for the design of miniaturized superconducting devices.

14. SUBJECT TERMS	15. NUMBER OF PAGES
Low Temperature, Superconductivity, Magnetoresistance	24
	16. PRICE CODE

17. SECURITY CLASSIFICATION OF REPORT	18. SECURITY CLASSIFICATION OF THIS PAGE	19. SECURITY CLASSIFICATION OF ABSTRACT	20. LIMITATION OF ABSTRACT
Unclassified	Unclassified	Unclassified	UL

NSN 7540-01-280-5500

Standard Form 298 (Rev. 2-89)
Prescribed by ANSI Std. Z39-18

TERMINAL REPORT
AFOSR 87-0148
PHYSICS and TECHNIQUES for the INVESTIGATION of the PROPERTIES of ULTRA SMALL SYSTEMS

J.M. Parpia, Principal Investigator
and
R.C. Richardson, Co-Principal Investigator
Department of Physics
and Laboratory of Atomic and Solid State Physics,
Cornell University
Ithaca, NY 14853-2501

Jeevak M. Parpia _____ May, 09, 1990.
Associate Professor of Physics

Robert C. Richardson _____ May, 9, 1990
Professor of Physics

ABSTRACT

This program is directed toward the study of transport and non-equilibrium thermal effects in diverse miniaturized systems at low temperatures. The research uses capabilities developed at Cornell to fabricate and probe the behavior of materials without affecting their internal structure. The techniques extend our ability to characterize materials as well as to understand the effects of technology used in patterning and fabricating small devices. The techniques developed in this research should prove to be useful for the non-destructive evaluation of the properties of materials as well as for the design of miniaturized superconducting devices.

Final Technical Report for activity under AFOSR Grant # 87-0148

A. Electron Scattering Rates in $CoSi_2$

Electrical conduction in thin $CoSi_2$ films grown on Si(111) wafers has been demonstrated [Hensel *et al.* (1985), Badoz *et al.*, (1987)] to exhibit a remarkable degree of specular scattering of the conduction electrons from the surfaces of the silicide film. The interface between the $CoSi_2$ layer and the silicon substrate is almost atomically smooth due to the close lattice match between the two materials [Gibson *et al.* (1982)]. As a consequence, although the electron mean free path is on the order of $\sim 500\mathring{A}$, the resistivity of the thin films does not show an increase until the thickness is decreased below $\sim 150\mathring{A}$. In addition, the $CoSi_2$ films exhibit a superconducting transition temperature on the order of 1.2K [Badoz *et al.*, (1987)], with the transition temperature being suppressed roughly as the resistivity increases. This suppression occurs for film resistivities of $\sim 30\Omega/\square$ rather than the critical resistance for the metal insulator transition $4000\Omega/\square$ [Anderson, (1958), Mott and Davis, (1979)].

Following the earlier results [Hensel *et al.* (1985)], the resistance increase observed with decreasing film thickness has been attributed to a quantum size effect, which is due to the discreteness of the momentum eigenstates in the direction perpendicular to the film. [Trivedi and Ashcroft, (1988)]

Our interest in this material system was captured by the high degree of specularity exhibited by it. However, it was evident that the measurements of the resistivity of the films was insufficient to specify the nature of the scatterers and the validity of whether the films were indeed exhibiting quantum size effects in their resistivity. There had also been no attempt to link the suppression of superconductivity and the increase in resistivity, despite the parallels in their signatures. Consequently, we have undertaken a comprehensive survey of the magnetoresistance of these samples to identify the nature and relative importance of the scatterers responsible for their transport signature.

By using high sensitivity resistance measuring techniques (with a resolution of better than 1 part in 10^5), we were able to discern a resistivity minimum at a few Kelvin for all the films with thickness less than $120\mathring{A}$. The zero field resistivity of these films appears to fall on the usual localization type of relation

$$\Delta R/R_{\square} = -R_{\square}\xi\alpha log(T/T_0)$$

with a coefficient α that appears to be ~ 1. Temperature sweeps at all fields up to 4T, reveal that this behavior is replicated with no additional field dependence. Our data is shown in figure 1.

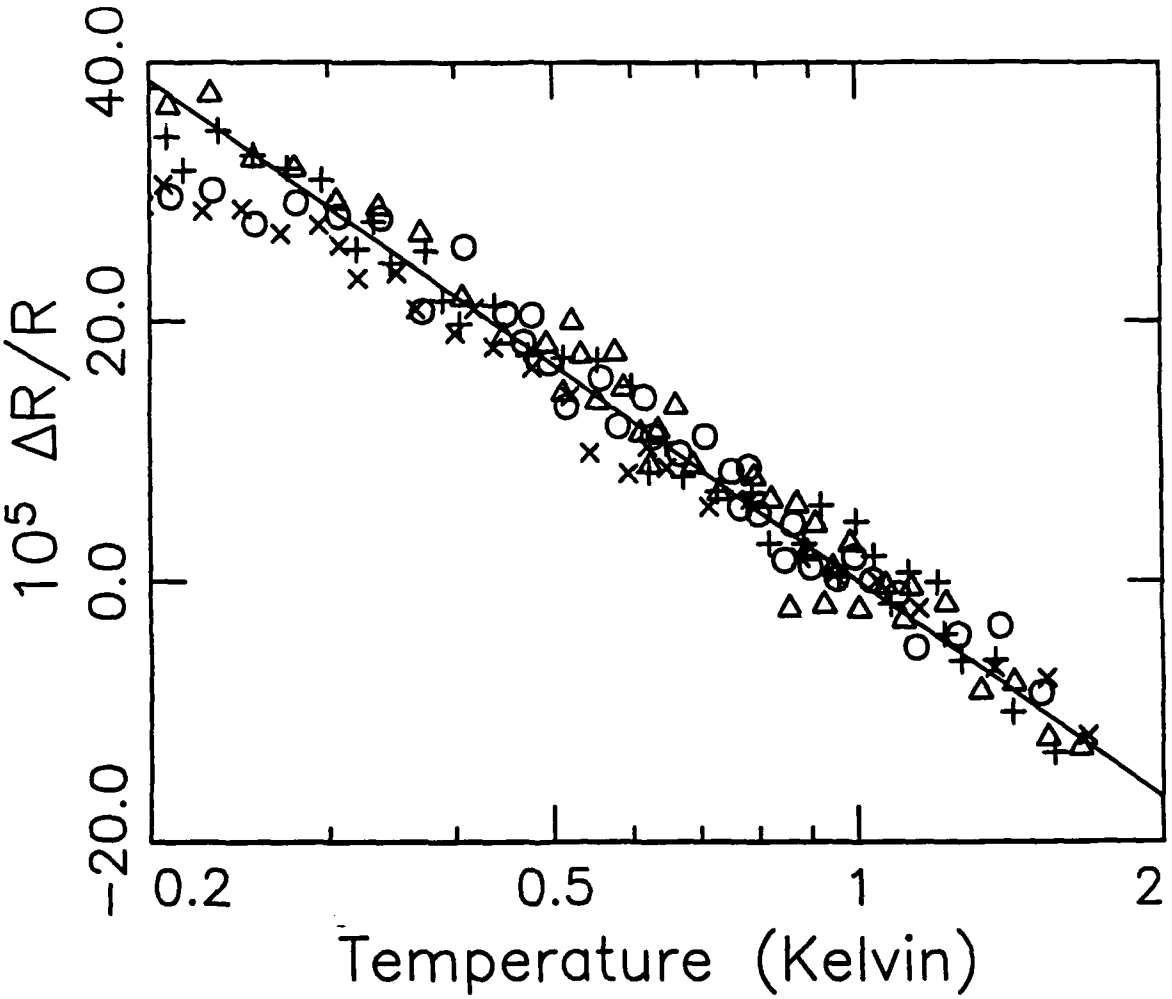

Figure 1. The temperature dependence of the resistance, $\frac{R(T,H)-R(1K,H)}{R}$, of the 6.4nm film in fields of 0.0(o), 0.1(+), 0.5(x), and 4.0T(△). A clear logarithmic dependence is seen with the coefficient showing no field dependence. The line is the theory (eq.1) for $\alpha_T = 1.0$.

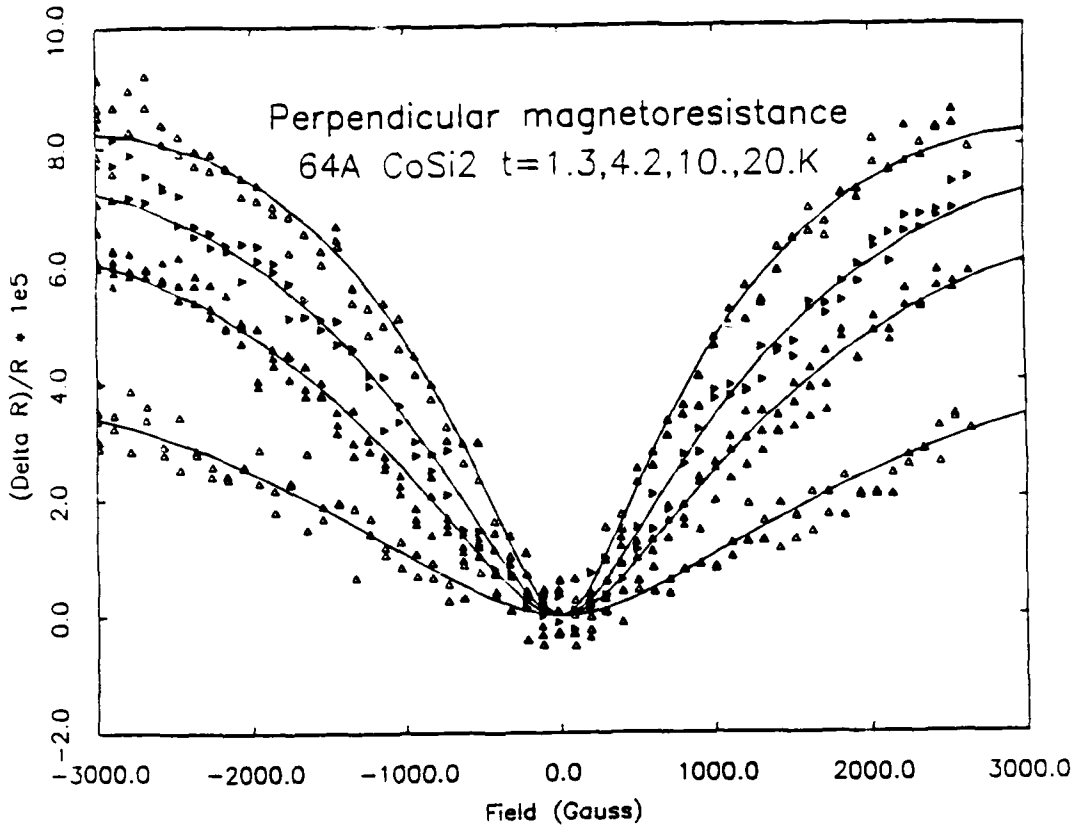

Figure 2. The resistance change of the same 64Å film in figure 1 vs. magnetic field at several temperatures, ranging from 20K (lowest data) to 1.3K (highest data). The lines drawn through the data are from fits to the theory (see text). Here R is the zero field resistance at any given temperature.

The appearance of a positive magnetoresistance at low fields implies that the dominant scattering rates are either spin- orbit or electron interaction. The magnitude of the magnetoresistance is temperature dependent saturating for temperatures below $\sim 1.2K$. Using diffusion constants for these films as determined from the depression of the transition temperature (or in the case of the thinnest films which did not exhibit a superconducting transition, their free electron value), the magnetoresistance curves could be fit with only one parameter, the phase breaking scattering rate. The data are shown in figure 2,

together with the fits obtained from the theoretical fitting procedure of Altshuler *et al.* (1987).

These results reveal for the first time that there is a substantial temperature independent scattering rate as shown in figure 3, and that this rate is larger for the thin films, indicating the presence of magnetic scattering in these films. While such magnetic scattering is clearly important in the suppression of the superconducting transition temperature its magnitude is not large enough to produce the degree of suppression of the transition temperature as observed in our thin films. However, the magnitude of suppression of T_c is rather similar to that observed by Badoz *et al.* (1987).

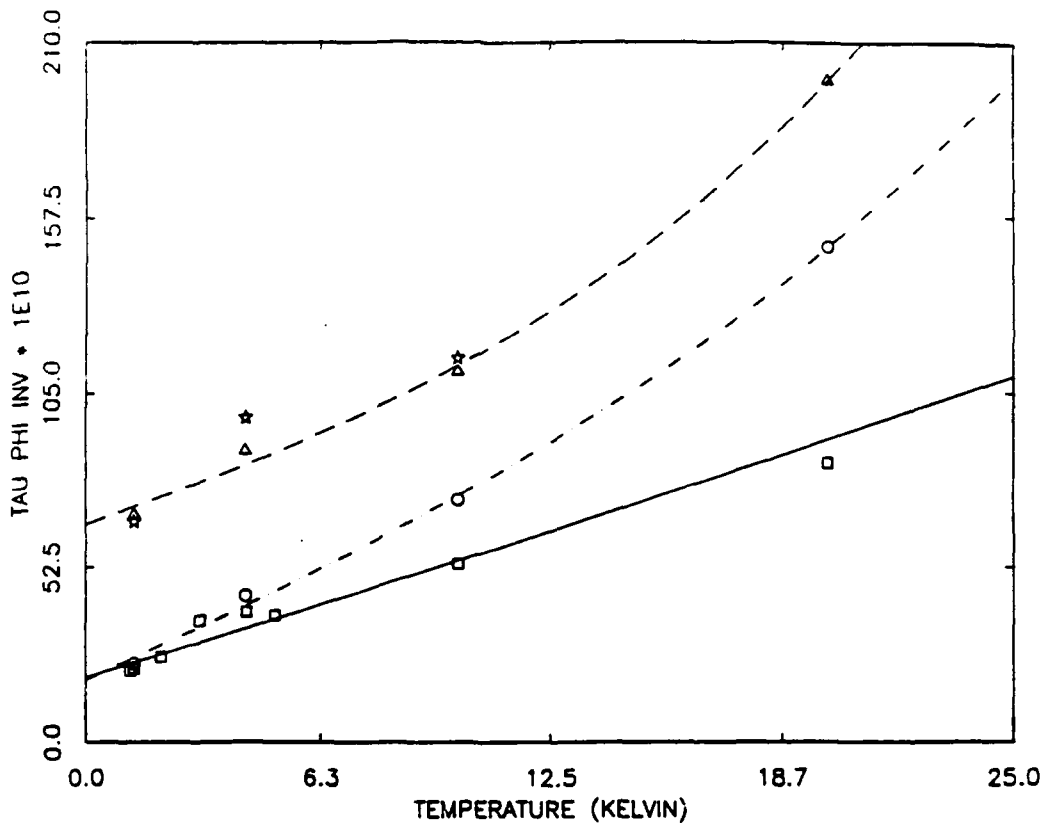

Figure 3. The phase breaking rate vs. temperature for films of thickness 120Å (boxes), 84Å (open circles), 64Å (triangles), and 39Å (stars). The lines are fits to the form AT + BT^3 + C.

To summarize, our measurements have revealed the presence of additional magnetic scatterers in thin $CoSi_2$ films, whose number increases with the decrease in film thickness. It is probable that there is unreacted Cobalt present in these films (as alluded to in Badoz *et al.*, 1987). The presence of these scattering sites will certainly play a role in the suppression of superconductivity.

B. Size Effects in Thin Free Standing and Supported Films

We have fabricated films and wires with dimensions small enough to restrict the excitation of thermal phonons below 4K in order to expose finite size effects due to the reduction of the dimensionality of phonons. To date, the films that we have studied have been made from aluminum. However, there is no intrinsic restriction on the material usable in this process.

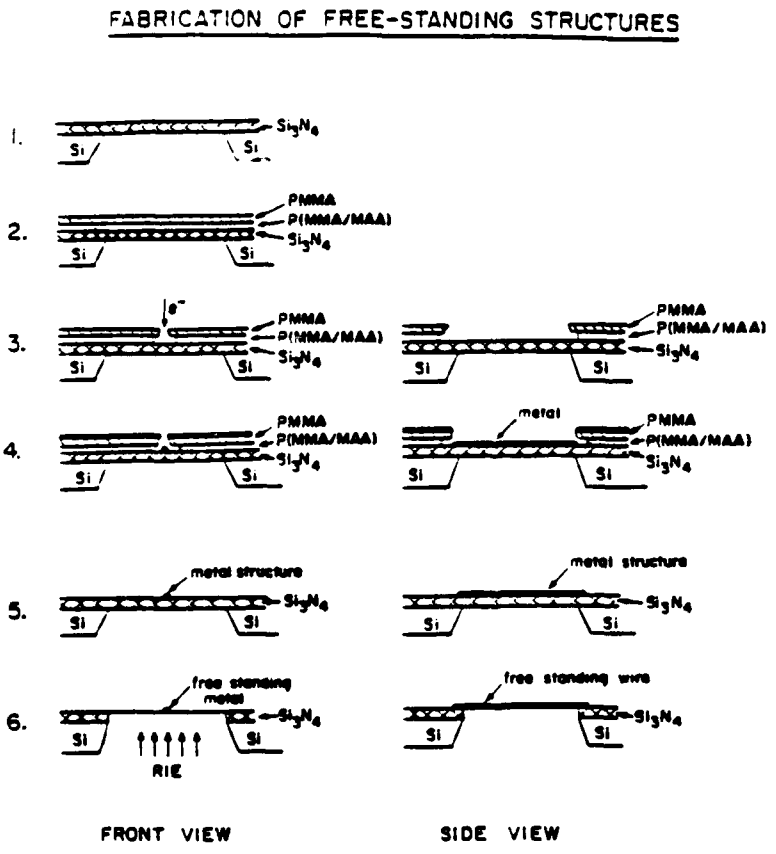

Figure 4. Schematic of the fabrication process used to produce free standing structures.

The process we have developed is illustrated schematically in figure 4. Some of the techniques used are well established methods of sample fabrication for quantum transport

studies [Prober, (1983)]. The starting material is a standard < 100 > silicon wafer with silicon nitride (Si_3N_4) deposited on both sides by low pressure chemical vapor deposition.

1. The silicon nitride membrane is made by patterning the nitride film on reverse side with photolithography and reactive ion etching, followed by wet etching in KOH solution.

2. Two layers of electron beam resist ((PMMA) polymers on top of P(MMA-MAA) copolymers) [Hu *et al.*, (1981); Hatzakis, (1979)] are spun on the membrane. For larger features, simple photolithography using commercial photoresist is used.

3. Electron beam lithography (exposure and development) defines the structure shape and size. If photolithography is used, this step is performed through an exposure by UV aligner followed by development.

4. Metal deposition by thermal or electron beam evaporation.

5. Lift-off resist by appropriate solutions. Well-defined metal structures are left on membrane.

6. Reactive ion etching (RIE) from below removes the membrane, leaving free-standing metal structures.

The first feature to note is that the process is independent of sample geometry. Any structure (from thin wires to wide films) which can be patterned onto the nitride window area can be made free-standing. The nitride window can be as large as $(250\mu m)^2$. We have successfully made free-standing 13 nm thick aluminum films up to $150\mu m$ wide and 100 μm long, and also 50 nm thin wires up to $100\mu m$ long. The process is also material independent. Any metal film strong enough to support its own weight can be used. The use of a controlled precisely timed RIE from below means that the sample films and wires suffer minimal damage. So far we have fabricated samples from aluminum, gold and copper with success, and many other metals should be possible. Our flexibility in sample geometry and material are in direct contrast to those of other experimenters [Smith *et al.*, (1986, 1987) and Butenko *et al.*, (1988)].

For a simple metal such as aluminum, the results are very reproducible and the yield is usually better than 90%. All steps of the process - lithography, wet and dry etching, metal deposition, and so on, employ standard microfabrication techniques using equipment available at the National Nanofabrication Facility. Starting from a clean wafer coated with silicon nitride, it takes about 2-3 days to produce free-standing samples ready for measurement. Each wafer can comfortably accommodate more than 120 sample chips. This allows us to easily make samples with wide range of geometric parameters and with

many different materials, in enough quantities so that the 10% of samples lost to accidents, mishandling and general quality control are inconsequential.

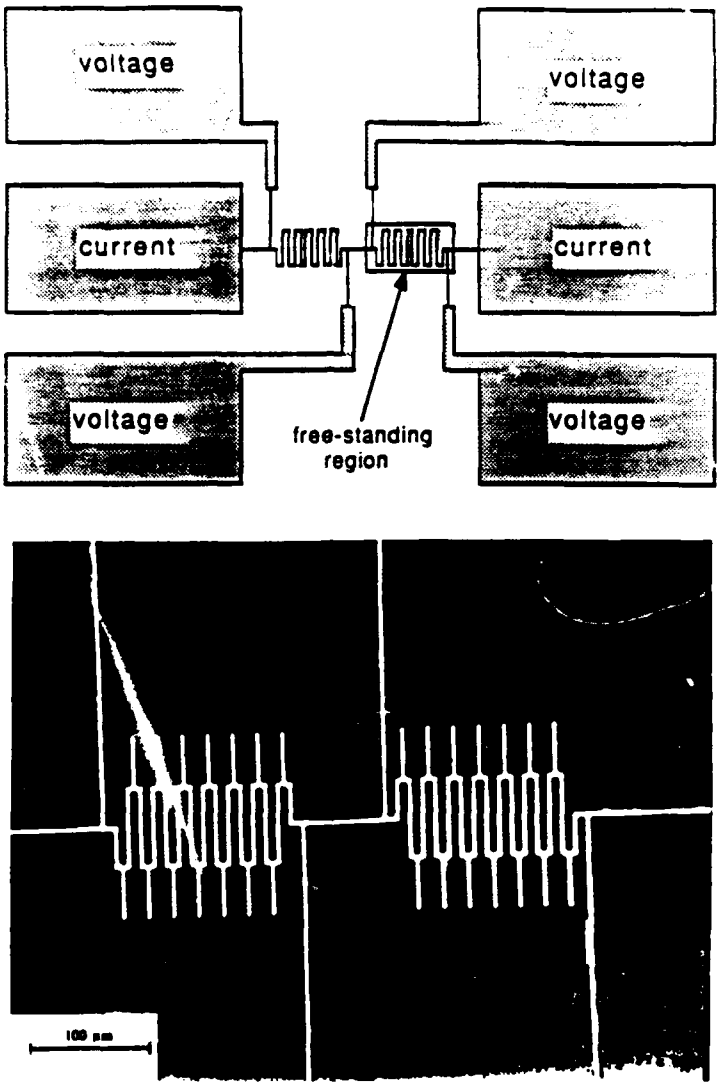

Figure 5. Schematic (top) and reproduction of micrograph (bottom), of 2D free standing microstructure with contiguous supported section. The finger like projections are mechanical supports for the free standing part of the current path. The line width is $\sim 5\mu m$.

Figure 5 shows a micrograph and a schematic of a typical sample. The pads, leads, and sample area consist of one continuous film of uniform material. Note that each sample

chip has identical sections on the bulk substrate and in the free-standing region. The sample strip is made into a meander path to maximize resistance for more sensitive magnetoresistance measurements. Each sample chip is mounted on a T0-5 header and a wire bonder is used to connect the header pins and sample pads. Figure 6 gives some close up views of free-standing gold wires (200 nm wide, 50 nm thick, 50μm long).

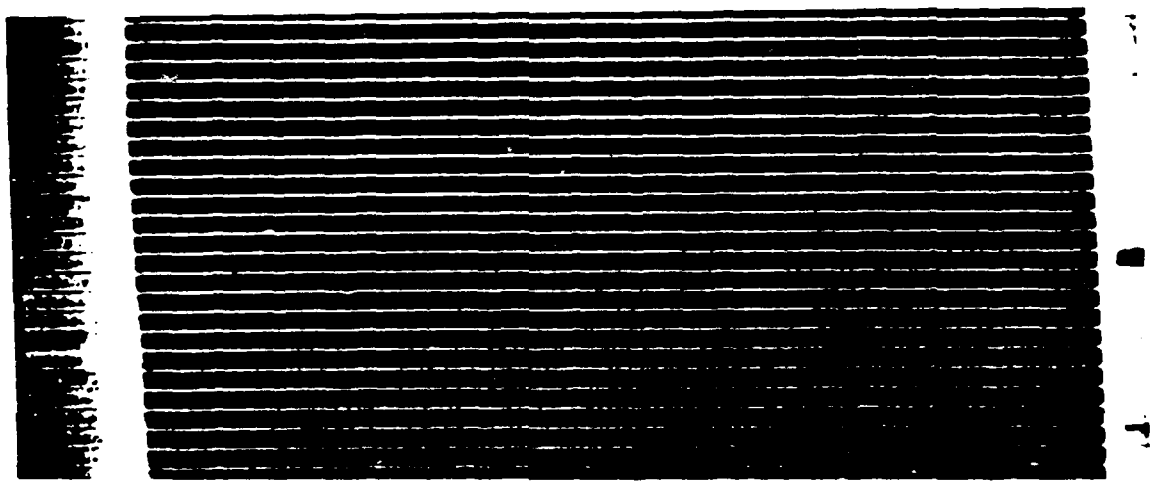

Figure 6. Electron micrograph of 2000$\AA$ wide $\times$500$\AA$ thick $\times$50μm long free standing gold microstructures. Wires with widths down to 500$\AA$ can be reproducibly fabricated.

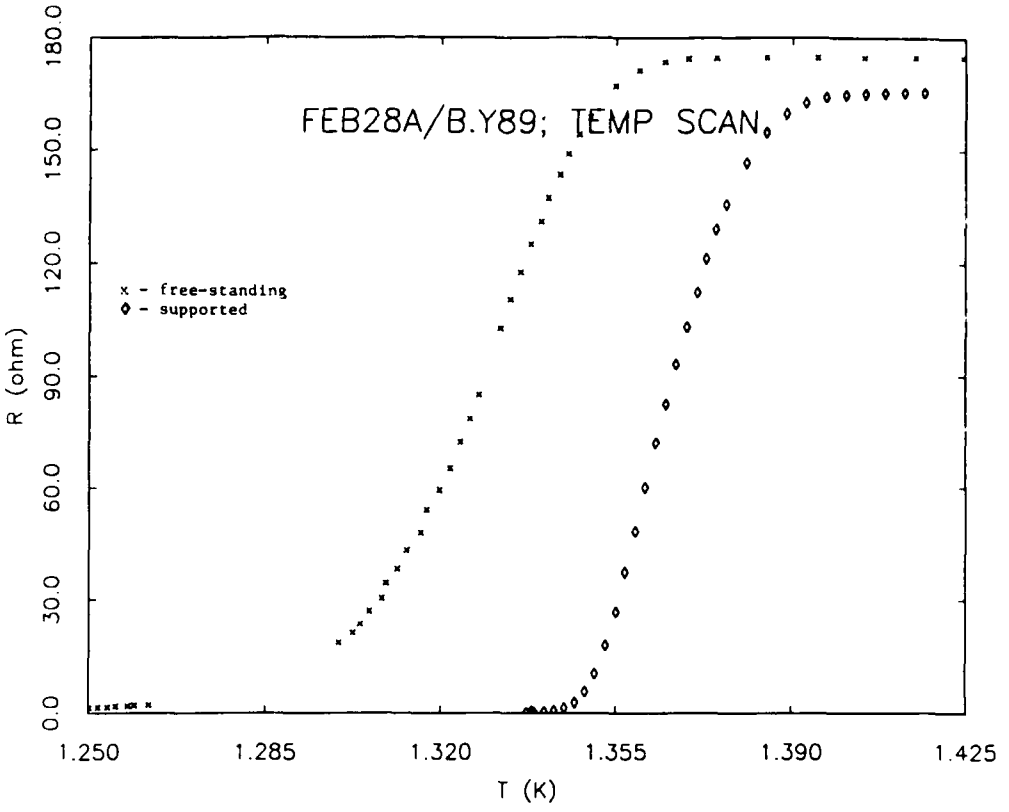

Figure 7. Typical Resistance vs Temperature data for free standing and supported 2D aluminum microstructures obtained in our preliminary studies.

Preliminary Results on Transport in Free Standing Films:

i) Shifts in T_c : Figure 7 shows typical data from some preliminary measurements obtained in the dilution refrigerator at the Microkelvin lab at Cornell. The samples were 25 nm thick Al films of $5\mu m$ width. All data showed clear differences in T_c between free-standing films (cross) and those on the bulk substrate (diamond). We have found that the transition temperature of the free standing segment is consistently reduced by 30 to 50mK below that of the corresponding supported segment. It is well known that many factors can cause changes in T_c in thin metal films [Overcash *et al.* (1983)]. By varying the thickness of the film, we observed that the overall transition temperature of both samples increased with decreasing film thickness. However, the relative depression of T_c in the free standing section was preserved. The most likely reason for such a depression is stress in the free-standing section induced by the differences in the thermal expansion coefficients of the aluminum and the silicon nitride substrate. Overcash *et al.* (1983) induced more than

50mK changes of T_c by stressing thin aluminum whiskers. Stress can therefore account for our observed shifts in T_c . However, it was also possible that the differences may have been induced by etch damage in removal of the substrate. (Such induced disorder is known to raise T_c in aluminum, contrary to our observed trend).

Consequently, we elected to characterize the effects of the RIE before continuing with this investigation [Kwong *et al.* (1989)]. Of course, changes in phonon population and density of states are also expected to influence T_c . But these effects cannot be isolated by simply measuring T_c .

ii) Fabrication Artifacts: The shifts in T_c and inelastic rates of the free-standing relative to supported structures could have been linked to process artifacts. In making the microstructure free- standing, reactive-ion etching (RIE) is used to remove the Si_3N_4 membrane support. Once the membrane is broken through by the plasma, the plasma comes into contact with the metal structure. Clearly, this is the most invasive part of the fabrication process.

We have directly addressed the issue of RIE-induced damage and its consequence on low-temperature transport. Specifically, low frequency resistance and magnetoresistance measurements were performed for 2D Al microstructures (on bulk substrates) which were purposely exposed to the identical RIE environment used to fabricate free-standing samples. Etching times were chosen to simulate reasonable RIE/microstructure interaction times during the preparation of free-standing structures. This study permitted us to isolate the effects of the etching step and to assess RIE processing artifacts which may result when fabricating free-standing microstructures.

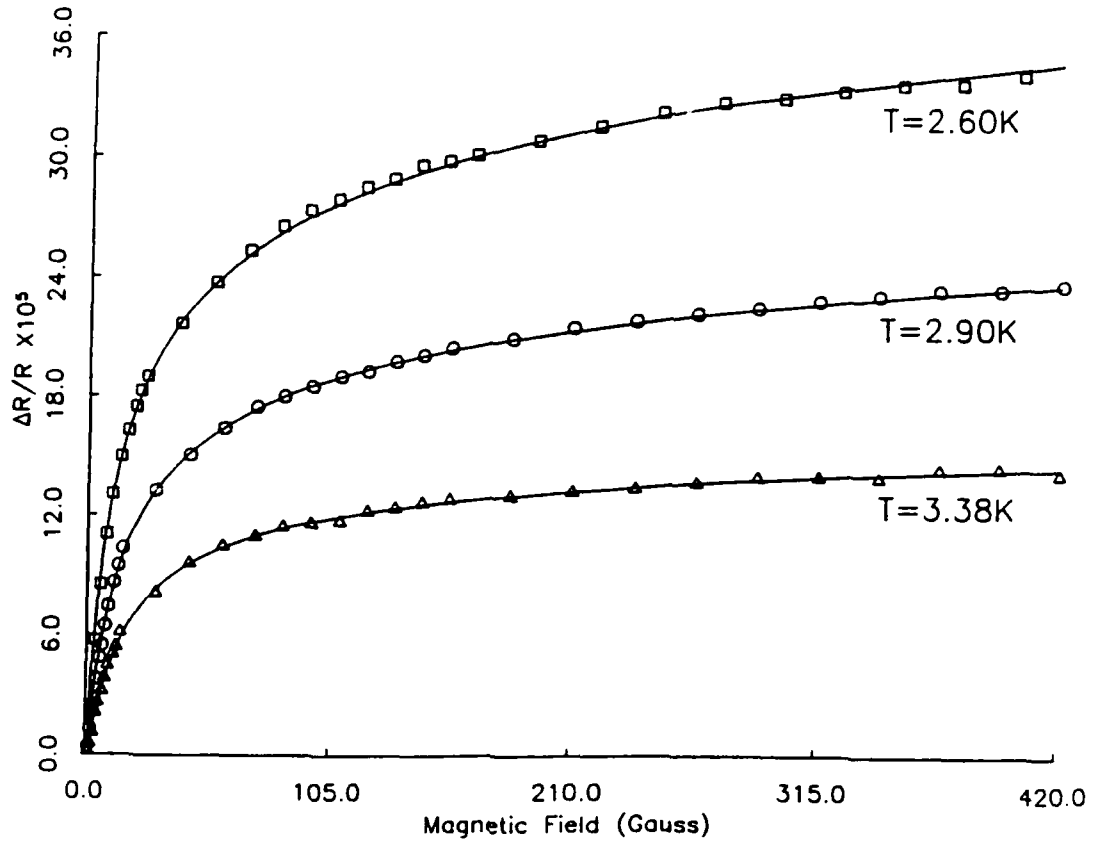

Figure 8. Typical magnetoresistance data obtained in our etching damage study. The solid lines are fits to the theory. Fits yield the scattering rates.

The resistance ratio and electron diffusion constant of the etched and unetched samples were found to be identical. The T_c of the etched sample was seen to be *enhanced* by $\sim$ 30 mK, contrary to the observations on the free-standing films. The magnetoresistance data was fitted to yield inelastic scattering rates between temperatures of 1.4 to 4 K. Figure 8 shows typical magnetoresistance data and the corresponding fits produced by the analysis at various temperature.

The result of this analysis, (Figure 9), indicates that there is no additional increase in the scattering rate due to the RIE, though a small constant increase in the inelastic scattering rate was produced upon oxygen descum. Most significantly, both etched and unetched samples exhibit precisely the same temperature dependence of the scattering rate, which is crucial to establishing the non-invasive nature of this process. Similar

magnetoresistance measurements have been carried out on free-standing samples, and these preliminary results are dealt with in the next paragraph.

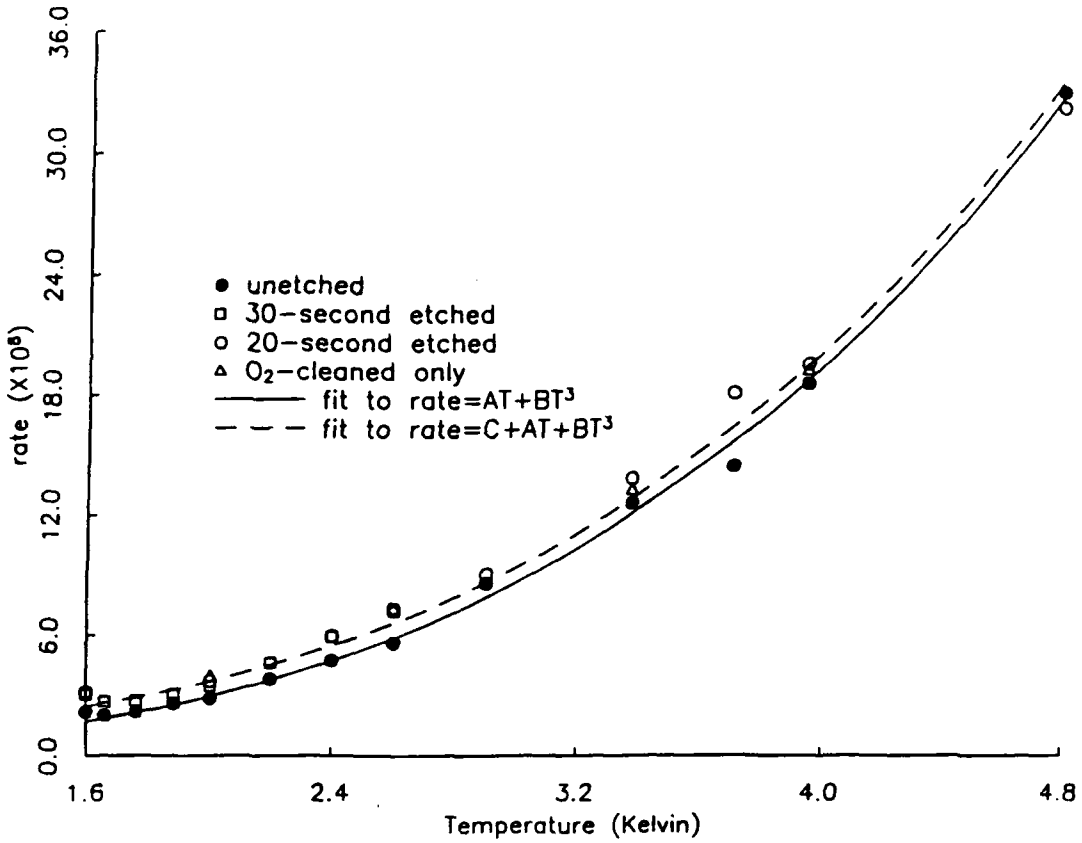

Figure 9. Inelastic scattering rate obtained from data similar to that of figure 8, in our etch damage studies. Note that the etched and unetched samples can be fit to the same power law.

iii) Inelastic Rates Differences: Preliminary measurements were carried out on free-standing and supported aluminum samples patterned using the same photo-mask as the etching studies described above. The samples were 250$\AA$ thick $\times$ 5μm wide, and spanned a temperature range between 1.4K and 2.5K. We have fitted the magnetoresistance data to the theory of superconducting fluctuations and weak localization. The results for the supported segment closely replicate those of the unetched sample discussed above. As expected, there is a clear increase in the inelastic scattering rate due to the superconducting fluctuations close to T_c . However, the free-standing section (which has a lower T_c) shows

a minimum in the scattering rate at a higher temperature than that of the supported segment, contrary to theoretical predictions.

The data collected thus far do not span a sufficient range of temperature to allow a meaningful comparison of the temperature dependences between the supported and free-standing sections,and is being extended to higher temperatures on new samples. These have a longer meander path and a correspondingly higher resistance. In our preliminary studies we found that the magnetoresistance became too small to measure at our low excitation levels. If the bridge excitation was increased, the transition temperature was found to increase indicating self heating. The longer samples have a higher resistance which produces a larger voltage for a given current. Small "buttresses" can be seen supporting the meander in figure 5. These serve as mechanical as well as thermal anchors for the film.

iv) Proximity Effect and Charge Imbalance Experiments: In the course of a preliminary experiment to examine the transition temperature of free-standing aluminum films for dimensional crossover effects, we observed a marked increase in the apparent resistance of the free-standing film at the onset of superconductivity.

The details of the experimental geometry (figure 5) are important in understanding the origin of this effect. A film of aluminum was deposited on a silicon nitride wafer which subsequently had the substrate removed from a small "window" section, leaving a portion of the film free-standing (Kwong et al., 1989). Voltage leads, fabricated at the same time from aluminum identical to the film under study were located across a section of the supported film. Voltage leads for the free-standing section were also fabricated simultaneously and were either free-standing (as shown in figure 5) or in close proximity to the window on the substrate. These voltage leads monitored the supported and free-standing sections respectively. (Note that the position of the voltage leads in the figure corresponds to the situation where there is no increase in the resistance).

Because of differential stresses, the transition temperature of the free-standing film section was found to be depressed by $\sim 30mK$ compared to the supported film sections. We found that the resistive transitions of the free-standing and supported film sections (circles and triangles respectively; see figure 10) in this configuration showed nearly identical widths, but if the voltage leads were supported, the resistance of the free-standing section showed a $\approx 10\%$ increase at the onset of superconductivity in the supported section (figure 10). When the voltage leads for the free-standing section were fabricated so as to be free-standing as well (figure 5), the resistance of both sections monotonically decreased near

the transition (figure 10). Furthermore, in the first configuration, when an overlayer of chromium was applied to the voltage probe, the resistive transition did not show the anomalous rise.

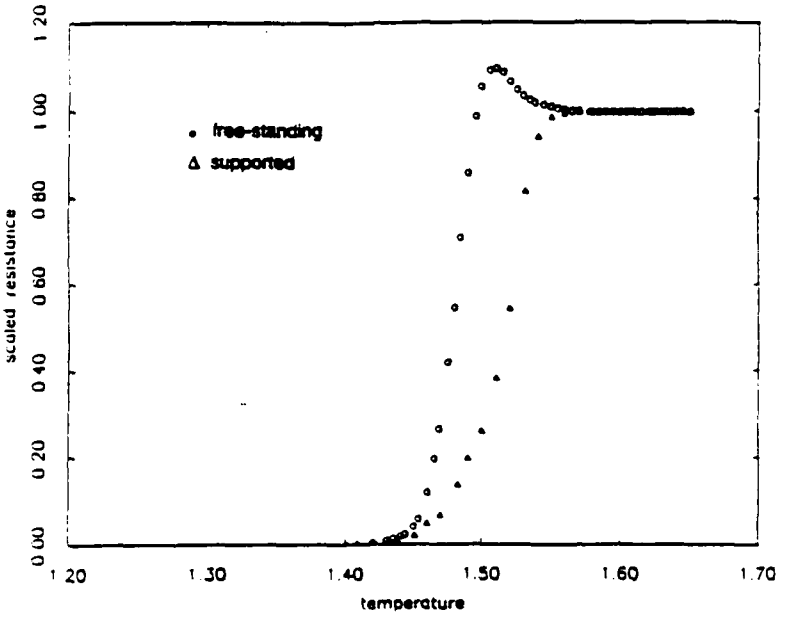

Figure 10a. The normalized resistance of free-standing (o) and supported (Δ) films of aluminum with the voltage leads located on a substrate in close-proximity to the "window" in the nitride layer.

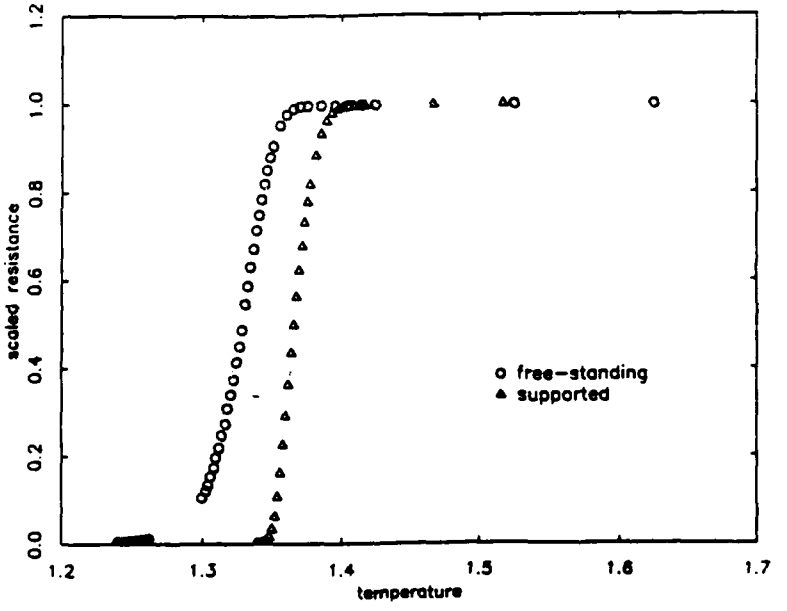

Figure 10b. The normalized resistance of free-standing (o) and supported (Δ) films of aluminum with the voltage leads also free-standing. Note the absence of the anomalous resistance increase for the free standing film.

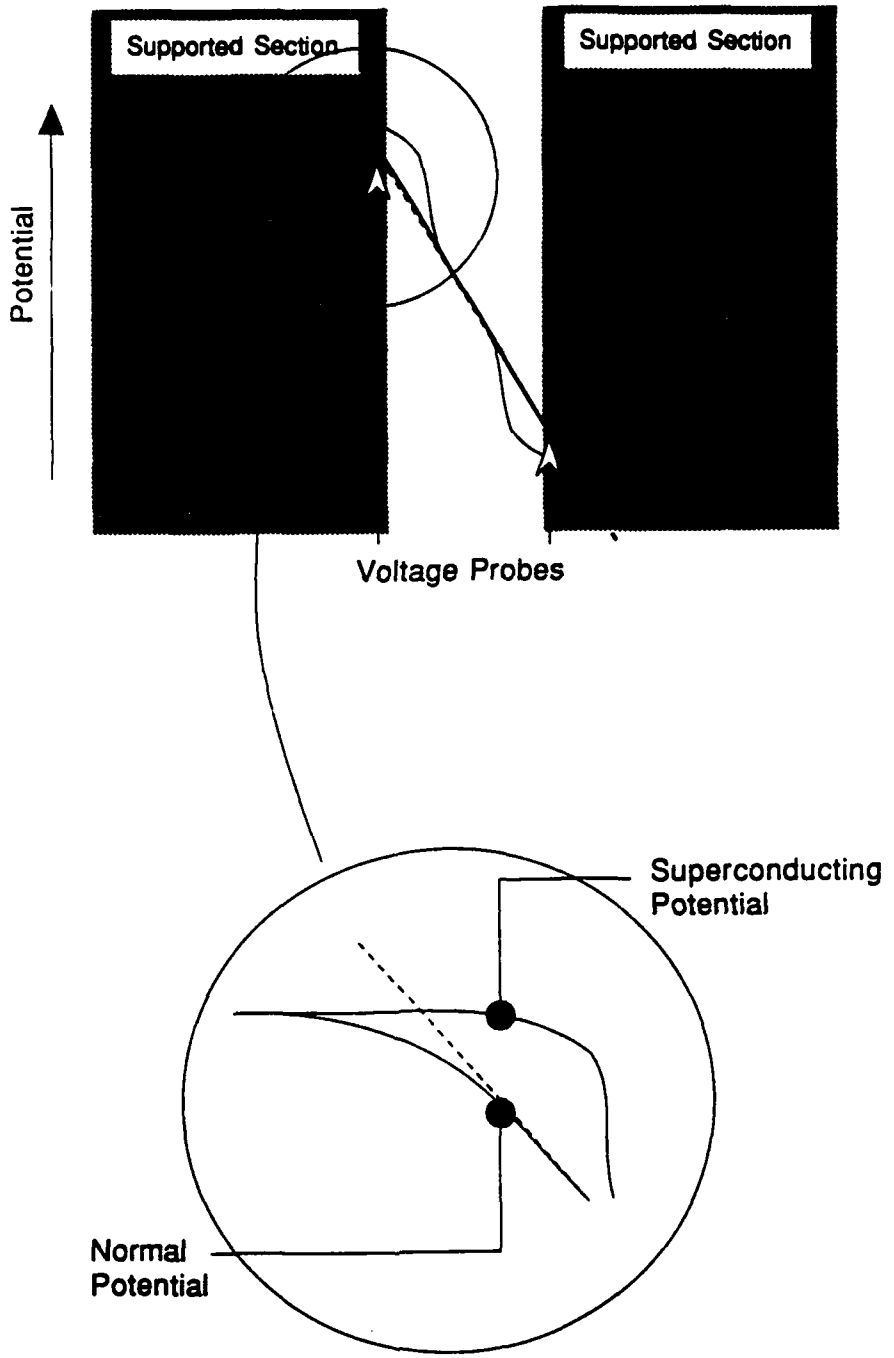

Figure 11. Schematic of the potentials near a free standing film with the T_c of the free-standing segment being lower than that of the supported segment. The dashed line represents the potential for both segments in the normal state. The superconducting and normal potentials are pinned at a distance corresponding to the quasiparticle lifetime from the junction. Superconducting voltage probes located at the large arrows sample the superconducting potential which is greater than that of the normal value. Normal electrodes located at the same point would register a small decrease in the potential.

This resistance increase is likely the consequence of non-equilibrium phenomena that exist at a superconducting-normal interface. To understand the effect we should refer to the potentials rather than the resistance. The nature of the voltage leads (whether the probes are normal or superconducting) determines which potential is sampled in the non-equilibrium region. Basically, close to T_c, the quasiparticles from the normal region are injected into the superconductor where they decay over a length scale corresponding to the quasiparticle lifetime. A normal voltage probe in the superconductor would sample the quasiparticle potential within this length scale. At a distance from the junction corresponding to the quasiparticle lifetime, the quasiparticles relax to their equilibrium distribution and consequently the quasiparticle and superconducting potentials are pinned to one another. Since the pair potential cannot vary within the superconductor, superconducting probes would sample this value anywhere in the non-equilibrium region. Thus superconducting voltage probes placed as shown in the schematic figure (11) would measure a potential higher than that of the normal state (shown as the dashed line). On the other hand, normal probes placed inside the free standing region would measure a potential slightly lower than that of the normal state. Finally, if the superconducting electrodes have an overlayer of chromium, then the superconductivity in the electrodes would be suppressed, causing the probes to measure the quasiparticle potential. Thus we have a simple qualitative explanation for our observation.

C. Energy Transport in Highly Disordered Conductors

This work was undertaken [Germain, (1989)] in order to obtain insight into phenomena affecting transport when the medium is disordered to the extent that the elastic mean free path is considerably shorter than the thermal phonon wavelength. Once again, the technique used to extract the scattering rates was to probe the electron-phonon interaction. However, instead of measuring and interpreting the magnetoresistance alone, a technique was devised to heat the electrons via an AC electric field applied at a frequency ω, and measure the response in the resistance at a frequency 3ω. This technique makes use of the

fact that in a highly disordered material, the resistivity increases at low temperatures as the log of T.

The samples were fabricated at NNF, and consisted of ion implanted Arsenic in Silicon. The doses were varied between 2.5×10^{14} to $10^{16}/cm^2$. By measuring the extent of the electron heating as a function of the electric field, the boundary resistance between the electrons and the phonon system could be measured. This is shown in figure 12 for three different samples. Using this data, the electron - phonon time constant could be determined using reasonable estimates for the electron area density and heat capacity. The electron phonon time constant could be calculated and showed a temperature dependence of $\tau T^{-3.4}$. This exponent is smaller than that expected for the dirty limit (T^{-4}), but the discrepancy is attributable to the effects of disorder which are not introduced into existing theories [Pippard (1955), Rammer and Schmid, (1986)].

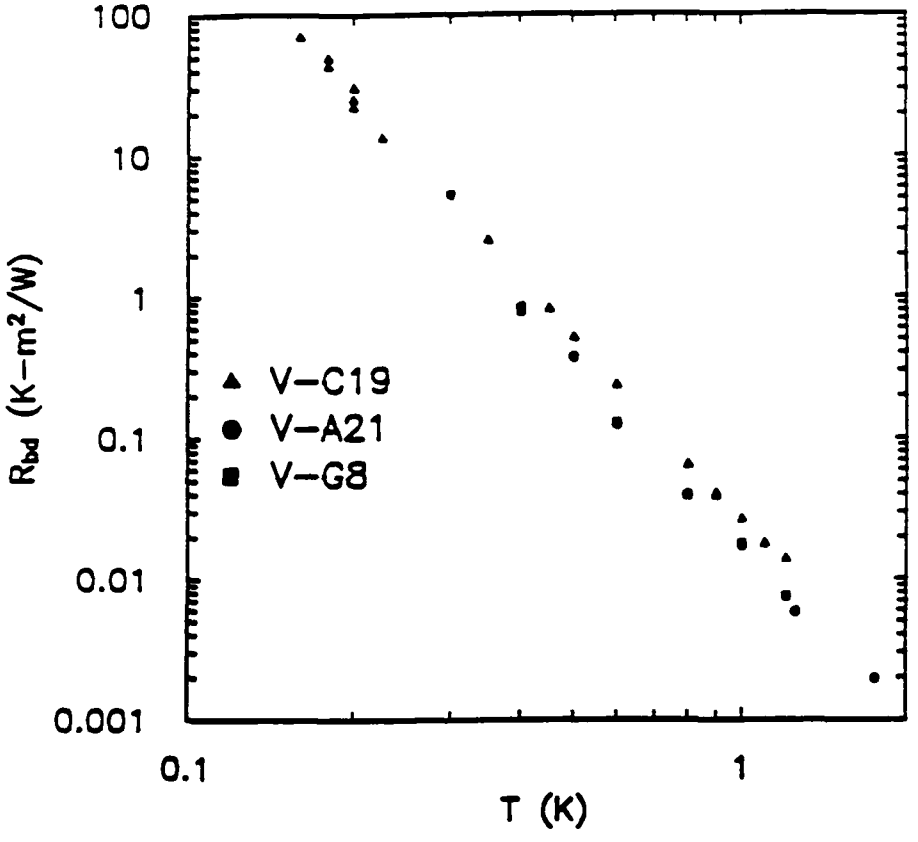

Figure 12. The thermal resistance extracted from the 3ω response data is plotted against the temperature. The data are expressed as boundary resistances, $R_t h \times$ Area. All

three samples display thermal resistances that vary as $R_b d \sim T^{-p}$, with the exponent, p, in the range between 4.3 and 4.5.

This work was mainly carried out on a grant from the SRC. However, the techniques used will be similar to those that we intend to employ for the electron heating work that is proposed in the next section. We undertake this research in order to understand the electron phonon scattering time in the dirty limit in metals whose phonon dimensionality will be reduced below 3D by confinement.

D. Apparatus

There are three cryostats which are currently available for this project. Two are dedicated for transport measurements, while the third is a dilution refrigerator cryostat which available essentially on demand for very low temperature work.

The first cryostat is a simple pumped pot apparatus which can be used either in a storage dewar or inserted in a relatively small research dewar which is equipped with a 7T superconducting magnet. In practice, we typically use the research dewar since it gives longer run times. The apparatus particularly allows us very fast cycle times and is used to take data at temperatures up to $\sim$ 20K. The lowest temperature accessible is $\sim$ 1.15K.

A new apparatus which has been completed recently has a continuously filled ^{3}He pot and 1K pot. This is a more complex cryostat which permits a greater degree of flexibility, particularly useful in measurements on superconductors down to 0.35K. It is equipped with a RF SQUID for use in low noise measurements, and with a low field magnet which is needed for magnetoresistance studies. A larger experimental volume and better wiring with nearly the same cycling time for cool-downs mean that this cryostat will be used most frequently in the near future

Finally, we have almost continual access to a top loading dilution refrigerator, which is particularly useful for studies of low temperature log T resistivity behavior in thin samples. Here the cycle time is relatively short, but the top loading feature limits the size of the samples and the number of leads available to monitor the sample. Experiments can also be mounted in the large space below the mixing chamber, but as yet no magnet is available for this region.

The experiments have been typically mounted on a TO5 pattern transistor mount, which is machined from copper so as to avoid magnetic materials present in commercial

holders. The TO5 package can be dismounted and remounted by push pins with no further handling for cool down on the top loading cryostat as well as on the smaller apparatus. In view of some of the experiments that we will be undertaking, we will likely have to modify the arrangements available on the top loading apparatus to accommodate at least two extra leads. There is of course no practical limit on the leads on the ^{3}He cryostat.

Data acquisition and temperature control is performed by two on-line PDP11-73 computers which we use on the different cryostats. Most of the thermometry used relies on calibrated Germanium and Carbon Glass resistors which are monitored by a four wire resistance bridge. The magnetoresistance and localization data are obtained using four wire bridges (Linear Research LR 400). However, some of the measurements of the thin film and wire samples show evidence for heating due to the excitation levels in these bridges. We are currently working on a version of the "Anderson" bridge [Anderson, 1972, Richardson & Smith, 1987] to allow us to read out the resistance using a low noise lock-in amplifier in conjunction with a low noise AC current source and nulling ratio transformer. The successful implementation of this bridge should allow us to lower the self heating by a factor of 100.

References

Altshuler, B. L., A. G. Aronov, M. E. Gershenson, and Y. V. Sharvin, Sov. Sci. Rev. 9, 223 (1987).

Anderson, A. C., Temperature **4**, 773, 1972.

Anderson, P. W., Phys. Rev. **109**, 1492, 1958.

Badoz, P. A., A. Briggs, E. Rosencher, F. Arnaud d'Avitaya, and C. d'Anterroches, Appl. Phys. Lett. **51**, 169, 1987.

Butenko, A. V., E. I. Bukhshtab, V. Yu. Kashvin, and Yu. F. Kamnik, Sov. J. Low Temp. Phys. **14**, 233, (1988).

Germain, R. S. "Energy Transport in Highly Disordered Conductors", Ph.D. Thesis, Cornell University, 1989.

Gibson, J. M., J. C. Bean, J. M. Poate, and R. T. Tung, Appl. Phys. Lett. **41**, 818, 1982.

Hatzakis, M., J. Vac Sci. Tech. **16**, 1984, 1979.

Hensel, J. C., R. T. Tung, J. M. Poate, and F. C. Unterwald, Phys. Rev. Lett. **54**, 1840, 1985.

Hu, E. L. and L. D. Jackel, IEEE Trans, Elec. Dev. ED-28, 1978,1981.

Kwong, Y. K., K. Lin, P. Hakonen, J. M. Parpia, and M. S. Isaacson, J. Vac Sci Tech., to be published, 1989.

Mott, N. F., and E. A. Davis, "Electron Processes ir Non-Crystalline Materials" Clarendon Press, Oxford, 1979.

Overcash, D. R., T. Davis, J. W. Cook, Jr., and M. J. Skove, Phys. Rev. Lett. **44**, 287, 1981.

Prober,D. E., Percolation, Localization, and Superconductivity, NATO ASI B, vol. 109, ed. A. M. Goldman and S. A. Wolf, Plenum Press, New York, 1983.

Pippard, A. B., Phil. Mag. **46**, 1104, 1955.

Pippard, A. B., Rep. Progr. Phys. **23**, 176, 1960.

Pippard, A. B., "Magnetoresistance in Metals", Cambridge University Press, 1989.

Rammer, J. and A. Schmid., Phys. Rev. B **34**, 1352, 1986.

Santhanum, P., S. Wind, and D. E. Prober, Phys. Rev. B **35**, 3188, 1987.

Smith, C. G., and M. N. Wybourne, Sol. St. Comm. **57**, 411, (1986).

Smith, C. G., H. Ahmed and M. N. Wybourne, J. Vac. Sci. Tech. **5**, 314, 1987.

Strongin, M., O. F. Kammerer, and A. Paskin, "Basic Problems in Thin Film Physics" Int. Symp., ed. R. Niedermayer and H. Mayer, Clausthal-Gottingen, 1965.

Trivedi, N. and N. W. Ashcroft, Phys. Rev. B **38**, 12298, 1988.

Van Duzer, T., and C. W. Turner, "Principles of Superconductive Devices and Circuits", Elsevier, 1981.

Publications

1. Kwong, Y.K., K. Lin, P. Hakonen, J.M. Parpia and M.S. Isaacson, "The Application of Reactive Ion Etching in Producing Free Standing Microstructures and its effects on Low Temperature Electrical Transport." J. Vac. Sci. Tech. B, 7, 2020 (1989).
2. DiTusa, J.F., J.M. Phillips and J.M. Parpia, "Quantum Transport in Ultrathin $CoSi_2$ Epitaxial Films." submitted to Applied Physics Letters.
3. Lin, K., Y.K. Kwong, M.S. Isaacson ed. J.M. Parpia "Aluminum Thin Films in the In-Place Modulated Superconducting Structures." submitted to Proceedings of LT XIX.
4. DiTusa, J.F., J.M. Parpia and J.M. Phillips. "Low Temperature Transport in Epitaxial $CoSi_2$ Films." submitted to Proceedings of LT XIX.